Hematopoietic cells maintain hematopoietic fates upon entering the brain

Mei Massengale,[1] Amy J. Wagers,[1] Hannes Vogel,[1] and Irving L. Weissman[1,2]

[1]Department of Pathology and [2]Department of Developmental Biology, Stanford University School of Medicine, Stanford, CA 94305

Several studies have reported that bone marrow (BM) cells may give rise to neurons and astrocytes in vitro and in vivo. To further test this hypothesis, we analyzed for incorporation of neural cell types expressing donor markers in normal or injured brains of irradiated mice reconstituted with whole BM or single, purified c-kit$^+$Thy1.1^{lo}Lin$^-$Sca-1$^+$ (KTLS) hematopoietic stem cells (HSCs), and of unirradiated parabionts with surgically anastomosed vasculature. Each model showed low-level parenchymal engraftment of donor-marker$^+$ cells with 96–100% immunoreactivity for panhematopoietic (CD45) or microglial (Iba1 or Mac1) lineage markers in all cases studied. Other than one arborizing structure in the olfactory bulb of one BM-transplanted animal, possibly representing a neuronal or glial cell process, we found no donor-marker–expressing astrocytes or non-Purkinje neurons among >10,000 donor-marker$^+$ cells from 21 animals. These data strongly suggest that HSCs and their progeny maintain lineage fidelity in the brain and do not adopt neural cell fates with any measurable frequency.

CORRESPONDENCE
Amy J. Wagers:
amy.wagers@joslin.harvard.edu

Abbreviations used: CNS, central nervous system; EGFP, enhanced GFP; GFAP, glial fibrillary acidic protein; HSC, hematopoietic stem cell; KA, kainic acid; KTLS, c-kit$^+$Thy1.1^{lo}Lin$^-$Sca-1$^+$; PB, peripheral blood; WBM, whole BM.

Much has been published in the past few years regarding the potential plasticity of hematopoietic stem cells (HSCs). In particular, multiple reports have suggested that rodent and human BM cells and BM HSCs can acquire neural cell fates both in vitro and in vivo (1–16). Several mechanisms have been postulated to explain this phenomenon: (a) HSCs, as a major stem cell component of BM grafts, may "transdifferentiate" to generate neurons or neuronal precursors; (b) BM HSCs may dedifferentiate to generate pluripotent stem cells with broad differentiation potential, and these cells are then capable of giving rise to neurons; (c) in addition to HSCs, BM may harbor tissues specific neuronal precursor cells, or pluripotent stem cells, that are directly capable of homing to and engrafting within the brain to generate mature neurons upon transplantation; and (d) apparent transdifferentiation from transplanted BM or HSCs may occur via cell fusion, likely between committed neural lineage cells and differentiated mature myeloid cells from the blood (for review see reference 17). Given the serious implications of possible BM or HSC contributions to neuronal lineages, both in the laboratory and for clinical medicine, rigorous analysis of claims of HSC plasticity in the neuronal milieu is clearly essential to clarify this apparent controversy.

Using confocal microscopy, we performed immunofluorescence analysis of brains harvested from mice previously irradiated and transplanted with whole BM or single, purified c-kit$^+$Thy1.1^{lo}Lin$^-$Sca-1$^+$ (KTLS) HSCs. Donor BM and HSCs were isolated from transgenic mice in which enhanced GFP (eGFP) was driven by the β-actin promoter, such that all cells and tissues in these mice, except erythrocytes and hair, are constitutively and irreversibly marked by bright green fluorescence. For lineage analysis of donor-marker–expressing cells, we used CD45 as a marker for hematopoietic cells (18), Mac1 and Iba1 for microglia (19), NeuN for neurons (20), glial fibrillary acidic protein (GFAP) for astrocytes, and Calbindin for Purkinje cells. Analysis for coexpression of CD45 was essential in this study to assay for full conversion of donor hematopoietic cells to a nonhematopoietic fate. To evaluate the effect of selective pressures on the capacity of BM or HSC-derived cells to incorporate donor markers into the brain, we analyzed contributions from donor cells in transplanted but otherwise unmanipulated animals and in two models of brain injury/regeneration, as follows: (a) a hippocampal injury model using intraperitoneal injection of kainic acid (KA) to induce seizures and (b) running wheel exercise, known to in-

A.J. Wager's present address is Section on Developmental and Stem Cell Biology, Joslin Diabetes Center, Boston, MA 02215.

duce hippocampal neurogenesis (21, 22). Finally, we generated and analyzed, the in steady state and after injury to the brain, parabiotic mouse pairs, surgically joined such that they developed a common, anastomosed vasculature. These parabiosis experiments allowed analysis of possible neural contributions from any blood circulating cells, including mature and immature blood progenitor cells, and circumvented the requirement for irradiation, which, although necessary for BM or HSC transplantation, has been shown to ablate tissue-specific neuronal stem cells and inhibit neurogenesis by altering the microenvironment supporting stem cell proliferation (23–25).

Data collected from either transplanted or parabiotic animals indicate that cellular contributions from transplanted or circulating cells both in the steady state and after injury or induced neurogenesis are largely restricted to hematopoietic ($CD45^+$) and microglial ($Iba1^+$ or $Mac1^+$) lineages. Coexpression of donor markers with neural antigens and/or morphology was exceptionally rare, and detected almost exclusively among cerebellar Purkinje cells, which have been shown previously to acquire donor markers via cell fusion events (26–28). These data contrast with recent papers suggesting that BM cells normally adopt neural cell fates at low but detectable levels (1, 2, 4, 6, 8, 14), and suggest that HSC and their progeny maintain lineage fidelity within the central nervous system (CNS).

RESULTS

To assay the ability of cells derived from BM, HSCs, or circulation to engraft hematopoietic and neural lineages within the brain of recipient mice, we analyzed 21 individual animals that were engrafted with these cells after either irradiation and transplantation, or parabiosis. Initially, observations were made by standard immunofluorescence microscopy, and brains from 14 mice were further analyzed in detail using confocal microscopy. In all cases, donor cells and their progeny were derived from GFP-transgenic mice, which constitutively express GFP from the ubiquitous β-actin promoter, and were transferred into nontransgenic (GFP^-) histocompatible recipients. Each of the animals selected for study showed substantial engraftment of the peripheral blood (PB) by GFP^+ donor cells, with chimerism ranging from 5 to 98% of total PB leukocytes and including contributions to both the myeloid and lymphoid lineages (see Tables I–III). Some animals were subjected to brain injury by intraperitoneal KA injection before analysis. In animals that survived KA injury (~70% of treated mice), responses in the first 2 h after injection ranged between grade 2 (focal with myoclonic jerks/twitches) and grade 5 (secondarily generalized to bilateral tonic and clonic movements; see Materials and methods).

Generation of microglia from transplanted BM or HSCs or from circulating cells

Initial observations of GFP^+ cells identified in the brains of nontransgenic animals transplanted with GFP-expressing BM or HSCs revealed that the vast majority of these cells exhibited morphology typical of microglia. To confirm this hypothesis, we performed costaining of GFP with the microglial markers Iba-1 and Mac-1 (Table I and Figs. 1 and 2).

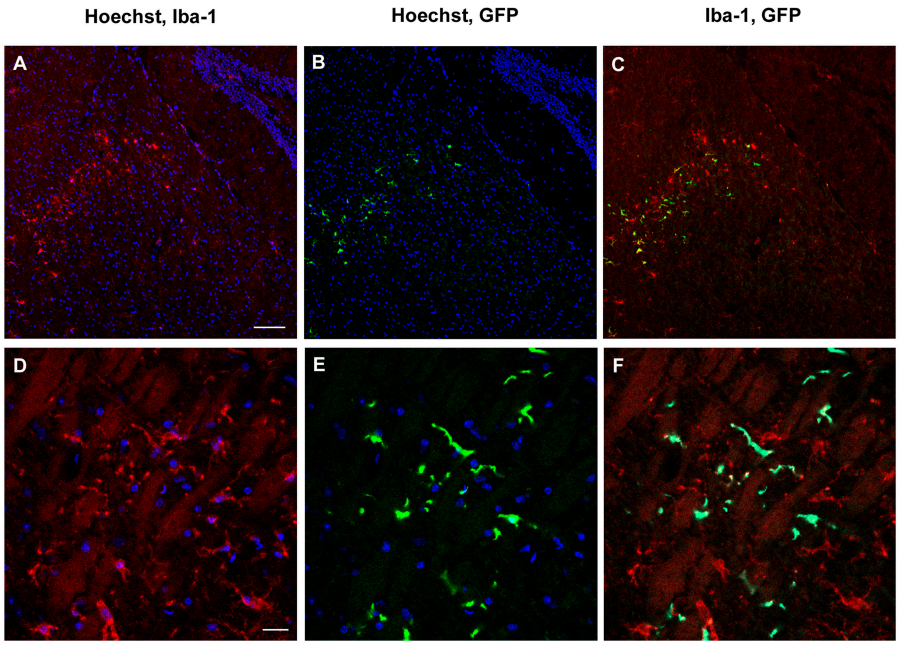

Figure 1. Confocal micrographs depicting microgliosis in the injured hippocampus of irradiated recipient mice, killed 8 d after KA injection, and 4.5 mo after transplantation with a single GFP^+ HSC. Tissue sections were costained with Hoechst 33342, anti–Iba-1 and anti-GFP antibodies. Images represent 10× (A–C) or 40× oil (D–F) magnification. Fluorescence shown is as follows: A and D: Hoechst 33342 (blue) and Iba-1 (red); B and E: Hoechst 33342 (blue) and GFP (green); C and F: Iba-1 (red) and GFP. Bar: A–C, 100 μm; D–F, 20 μm.

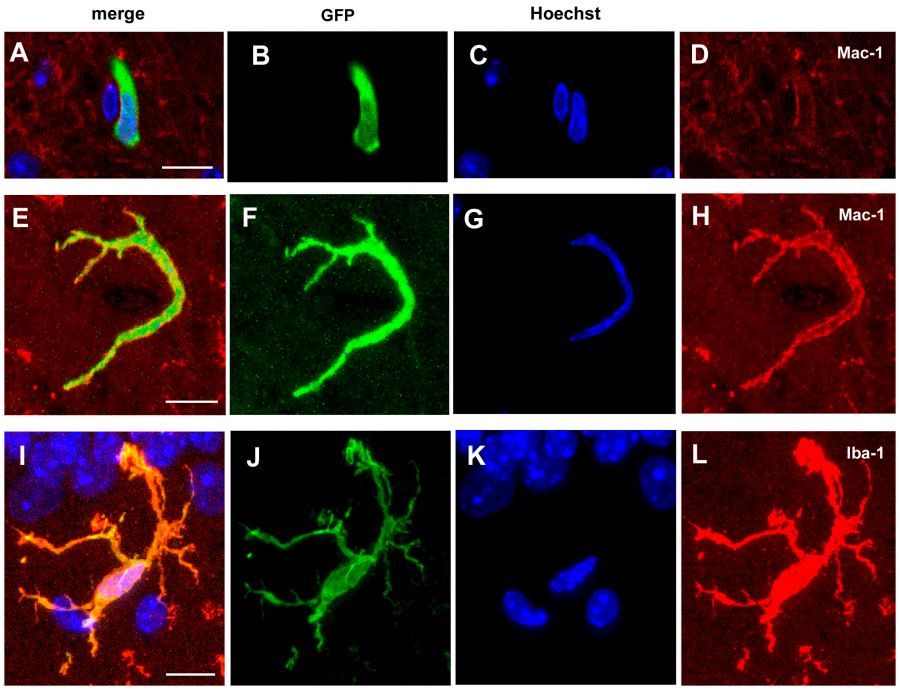

Figure 2. Laser scanning confocal images of microglia from brain tissue of a single HSC transplanted mouse killed at day 8 after KA injection (A–H) or a single HSC transplanted mouse transplanted and killed without additional brain injury (I–L). Tissues were stained with anti–Mac-1 or anti–Iba-1 antibodies (red); anti-GFP antibody (green); and Hoechst 33342 (blue). Fluorescence shown is as follows: GFP (B, F, and J); Hoechst 3342 (C, G, and K); Mac-1 (D and H); Iba-1 (L); merged (A, E, and I). Bar, 10 μm.

In all animals evaluated, the percent of donor-derived GFP^+ cells coexpressing microglial markers ranged from ~51 to 99%. The degree of contribution of transplanted cells to the generation of microglia appeared similar between animals transplanted with unfractionated BM cells or with purified KTLS HSCs, and between animals transplanted at birth or as adults (Table I). Treatment of animals with KA to induce hippocampal injury did not appear to increase the frequency of Iba-1–expressing GFP^+ cells (Table I), but did in some cases induce substantial microgliosis in the area surrounding the hippocampus; these microglial foci contained cells of both donor (GFP^+) and host (GFP^-) origin (Fig. 1). In general, although most GFP^+ cells found in the brains of BM- or HSC-transplanted mice appeared to be microglia, the overall contributions of such cells to the brain-resident microglial populations were quite low; donor-derived microglia comprised only 0.5–11.5% of resident microglia in the irradiation/transplant models (including recipients of whole BM [WBM] and of purified HSCs and despite the observation that in over half of the animals, contributions to PB leukocytes were >60%).

GFP^+ microglia were also observed in animals joined by parabiosis. Surgically joined parabiotic animals develop a common, anastomosed vasculature, with cross-circulation first detectable ~2–3 d after joining and ~50% mixing of blood elements achieved within ~10 d (29, 30). Furthermore, rapid and enduring cross-engraftment of BM cells, and particularly of BM HSCs, has been demonstrated in parabiotic mice joined for as little as 2 wk (30, 31). Analysis of nontransgenic animals that had been joined by parabiosis to GFP-transgenic partners revealed that ~17–43% of the GFP^+ cells found in the brains of these mice coexpressed the microglial marker Iba-1 (Table I). The overall contribution of GFP^+ cells to brain microglia in these animals was quite low (0.01–1.38% GFP^+ microglia), despite ~50% chimerism of cells in the PB of these mice (Table I). The lower frequency of GFP^+ microglia observed in parabiotic mice, as compared with transplanted animals, may suggest that irradiation-mediated destruction of existing brain-resident microglia facilitates engraftment by cells in the periphery, which ultimately derive from BM and HSCs. Consistent with the hypothesis that microglia are normally replaced from peripheral sources relatively infrequently, contributions of GFP^+ cells to the microglial pool were observed at greater frequency in animals joined for 3 or 9 mo (0.04–1.38% GFP^+ microglia), as compared with animals in which cross-circulation had only recently been established (0–0.02% GFP^+ microglia in mice joined for 9–15 d). Hippocampal injury induced by KA treatment did not appear to increase the rate of detection of GFP^+ microglia in parabiotic mice at these early time points (Table I).

Together, these data indicate that microglia are engrafted at low levels from BM cells after standard protocols of irradiation and transplantation, and from circulating cells after para-

Table I. Analysis of microglial marker expression by GFP$^+$ cells in brains of transplanted or parabiotic mice

Engraftment model	Animal no.	Age at transplant or parabiosis	No. of cells transplanted	Duration of survival after transplant/parabiosis	Injury model	Hematopoietic chimerism at death (% GFP$^+$ PB leukocytes)	Iba1$^+$ donor cells per section, mean ± SD (total cells analyzed: GFP$^+$Iba$^+$/GFP$^+$)	GFP$^+$ microglia per section, mean ± SD (total cells analyzed: GFP$^+$Iba$^+$/Iba$^+$)
							%	%
WBM transplant	1	newborn	10^6	9 mo	no injury	13	78.8 ± 2.2 (167/212, $n = 2$)	2.2 ± 0.8 (167/7,607, $n = 2$)
	2	newborn	10^6	9 mo	no injury	5	80.6 ± 7.0 (241/299, $n = 3$)	4.3 ± 2.3 (241/5,613, $n = 3$)
	3	adult	10^6	3 mo	no injury	88	92.3 ± 2.7 (886/960, $n = 3$)	11.5 ± 1.7 (886/7,697, $n = 3$)
	4	adult	10^6	3 mo	no injury	63	85.0 ± 2.3 (597/703, $n = 2$)	6.0 ± 0.5 (597/9,890, $n = 2$)
	5	adult	10^6	6.5 mo	KA	92	90.3 ± 5.5 (475/526, $n = 2$)	4.8 ± 1.8 (475/9,856, $n = 2$)
	6	adult	10^6	7 mo	KA	94	58.0 ± 19.2 (409/705, $n = 2$)	4.9 ± 0.6 (409/8,393, $n = 2$)
HSC transplant	7	adult	1	3 mo	no injury	10	93.1 ± 5.5 (54/58, $n = 4$)	0.5 ± 0.1 (54/10,865, $n = 4$)
	8	adult	1	3 mo	no injury	72	53.7 ± 23.8 (36/67, $n = 3$)	0.8 ± 0.03 (36/4,363, $n = 3$)
	9	adult	1	4.5 mo	KA	27	97.6 ± 4.7 (82/84, $n = 2$)	1.5 ± 0.7 (82/6,939, $n = 2$)
	10[a]	adult	1	9 mo	KA	98	91.0 ± 3.3 (343/377, $n = 2$)	7.2 ± 2.1 (343/4,755, $n = 2$)
	11	adult	100	4 mo	KA	88	99.3 ± 0.8 (279/281, $n = 2$)	4.7 ± 1.1 (279/5,598, $n = 2$)
	12	adult	100	7 mo	KA	47	58.1 ± 14.4 (864/1,488, $n = 2$)	10.7 ± 0.4 (864/8,230, $n = 2$)
Parabiosis	13	adult	NA	7 mo	no injury	22	42.8 ± 23.5 (62/145, $n = 3$)	1.4 ± 0.2 (62/3,302, $n = 3$)
	16	adult	NA	9 d	no injury	60.2	0	0
	14	adult	NA	9 d	KA	52	33.3 ± 70.7 (1/3, $n = 2$)	0.01 ± 0.1 (1/7,380, $n = 3$)
	15	adult	NA	16 d	KA	61	16.7 ± 11.6 (2/12, $n = 3$)	0.02 ± 0.03 (2/11,330, $n = 4$)
	17	adult	NA	3 mo	KA	41	20 ± 44.9 (3/15, $n = 4$)	0.04 ± 0.03 (3/7,733, $n = 4$)

[a]This animal received 2×10^6 unfractionated BM cells from a single HSC transplanted mouse.
NA, not applicable.

biosis. These cells most likely derive from HSCs and their progeny, as animals reconstituted by HSCs appear to show similar microglial chimerism as animals reconstituted by unfractionated BM cells. Such hematopoietic lineage microglia constitute the vast majority of cells expressing donor-markers found in the brains of transplanted and parabiotic animals.

CD45 immunoreactivity of microglial marker–negative population

As described before, in most mice, the vast majority of donor-marker–expressing (GFP$^+$) cells found in the brain after transplant or parabiosis coexpressed the microglial markers Iba-1 and/or Mac-1; however, some cells in these analyses failed to stain with these markers. To characterize further the population of GFP$^+$ cells that failed to stain with microglial markers, and particularly to evaluate the possibility that these represent blood cells of nonmicroglial lineage, we costained brain sections from WBM or HSC-transplanted mice with the panhematopoietic marker CD45 and Iba-1, or with CD45 and Mac-1, and analyzed the GFP$^+$ cells using confocal microscopy for expression of these hematopoietic and microglial markers. Consistent with earlier analyses (31), very few GFP$^+$ cells failed to costain in these assays. The frequency of donor-marker–expressing (GFP$^+$) cells coexpressing either CD45 and/or Iba-1 or Mac-1 ranged from ~96-100% for WBM-transplanted mice and from ~98.5–100%

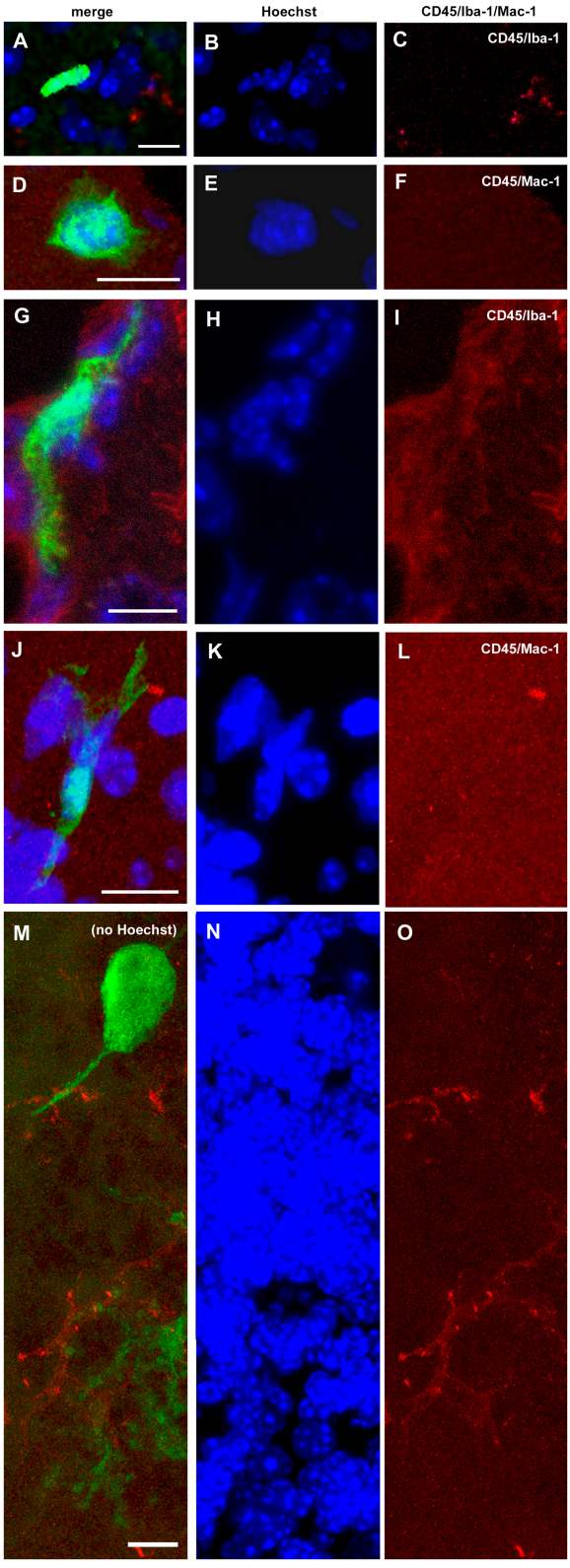

Figure 3. Representative laser scanning confocal micrographs of mouse brain cells negative for CD45 and microglial markers (Mac-1 or Iba-1). Animals were transplanted with single HSC (A–C) or whole BM (D–O). Tissues were stained with anti-CD45 and anti-Iba-1 (A–C and G–I, red) or anti-CD45 and anti–Mac-1 (D–F and J–O, red); anti-GFP (green); and Hoechst 33342 (blue). For A–C, CD45 and Iba-1 were detected using Alexa633 and Alexa594 dyes, respectively (C, merged image). Bar, 10 μm.

for recipients of a single HSC (Table II). Representative confocal micrographs depicting rare GFP$^+$ cells that failed to costain with hematopoietic and/or microglial markers are shown in Fig. 3. KA treatment did not appear to increase the frequency of detection of rare CD45$^-$/Iba-1$^-$ or CD45$^-$/Mac-1$^-$ GFP$^+$ cells (Table II).

No expression of neuronal and astrocyte markers by GFP$^+$ cells in transplanted or parabiotic mice

To characterize further the donor-marker–expressing (GFP$^+$) cells that failed to express either microglial markers or CD45, we costained sagittal brain sections with CD45 and Mac1, together with either NeuN (labeling neurons), Calbindin (labeling Purkinje cells), or GFAP (labeling astrocytes). As criteria for defining neural lineage cells, we required (a) absence of staining with the hematopoietic marker CD45 and (b) staining with NeuN or calbindin (neuronal) or with GFAP (astrocytic) or exhibition of distinctive morphology (Purkinje neurons only). A summary of the results of these analyses is given in Table III, with representative confocal micrographs shown in Figs. 4, 5, and 6. Consistent with previous papers (26–28, 31), a low frequency of GFP$^+$ Purkinje neurons was detected among cerebellar cells of a subset of transplanted mice (Table III and Fig. 6). However, among five WBM-transplanted, five HSC-transplanted, and two parabiotic animals analyzed, we observed no cells fulfilling the aforementioned criteria as donor-marker–expressing astrocytes and no cells qualifying as non-Purkinje neurons. Similar results were obtained using MAP2 instead of NeuN as a neuronal marker (unpublished data). Within the olfactory bulb of one animal transplanted as a newborn with GFP-expressing BM cells, we observed a GFP$^+$ arborizing process, which was negative for CD45 and showed possible partial colocalization of GFAP (Fig. 5). In several cases, we observed some candidate neuronal cells that, under lower magnification (40× oil), appeared to coexpress GFP and NeuN; however, when examined at higher power (100× oil), these cells exhibited atypical, cell surface localization of NeuN reactivity and coexpressed CD45 (Fig. 4). Therefore, these cells were excluded as bona fide neurons. Cell surface NeuN signals may arise due to nonspecific interactions between CD45$^+$ blood cell surface proteins and anti-NeuN antibody, as has been suggested in other studies (32). The appearance of NeuN$^+$ or GFAP$^+$ CD45$^-$ cells was not induced by KA injury or by enhancement of neurogenesis through the provision of a running wheel, nor did such treatments enhance the detection of GFP$^+$ Purkinje cells (Table III). Thus, other than one GFP$^+$ arborizing process, which was negative for CD45 and showed partial colocalization of GFAP (Fig. 5), no cells were found to simultaneously stain positively for NeuN or GFAP and negatively for both CD45 and Mac1 markers in any other animals, including the KA injured and parabiotic mice (Table III).

Table II. Frequency of GFP$^+$ cells in the brains of WBM or HSC transplanted mice failing to express hematopoietic or microglial lineage markers

Engraftment model	Animal no.	Age at transplant or parabiosis	No. of cells transplanted	Duration of survival after transplant/parabiosis	Injury model	Hematopoietic chimerism at death (% GFP$^+$ PB leukocytes)	GFP$^+$ nonhematopoietic cells (CD45$^-$Mac$^-$ or CD45$^-$Iba$^-$ cells/ total GFP$^+$ cells [%])
WBM transplant	1	newborn	10^6	9 mo	no injury	13	11/281 (3.9%)
	2	newborn	10^6	9 mo	no injury	5	4/167 (2.4%)
	3	adult	10^6	3 mo	no injury	88	2/128 (1.6%)
	4	adult	10^6	3 mo	no injury	63	1/282 (0.4%)
	5	adult	10^6	6.5 mo	KA	93	0/102 (0%)
HSC transplant	8	adult	1	3 mo	no injury	72	2/128 (1.56%)
	18	adult	1	5 mo	no injury	62	0/84 (0%)
	9	adult	1	4.5 mo	KA	27	0/90 (0%)

These data suggest strongly that BM-derived, HSC-derived, and circulating precursors do not normally contribute at detectable levels to neuronal or glial lineages in the adult brain.

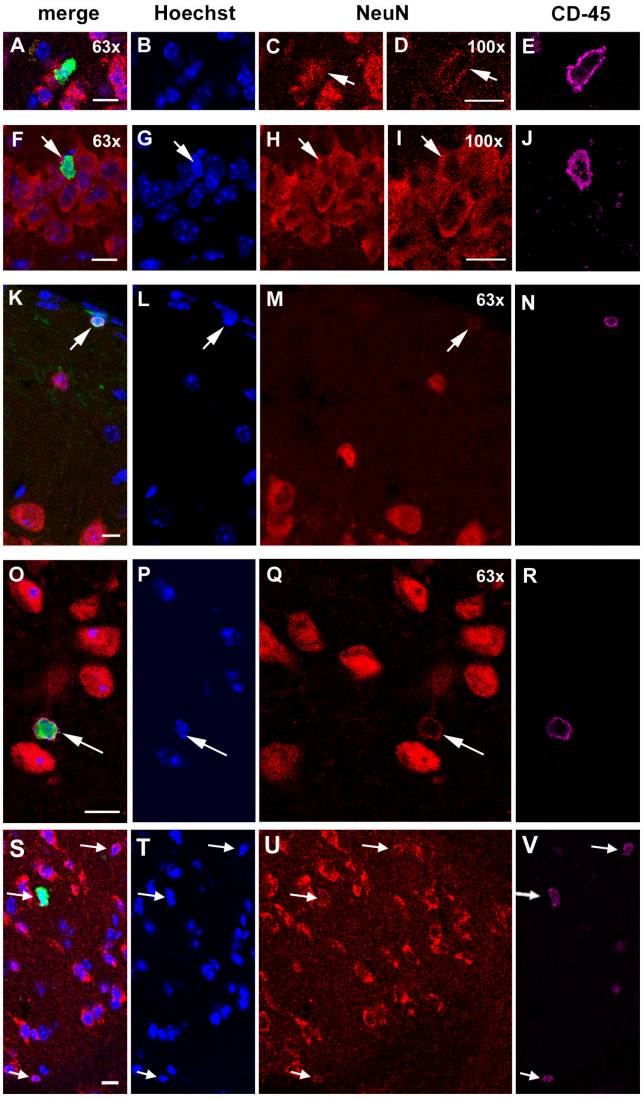

DISCUSSION

Derivation of microglia from HSCs

Historically, it has been debated whether HSCs or other components of BM primarily give rise to the microglial population in the brain (33–39). Our data clearly demonstrate that microglia can be generated in adult animals from direct transplant of a single HSC. In fact, we found that the majority of cells derived from BM or from HSCs that enter the brain after transplant differentiate to become microglia, with between ~54 and 98% of donor-derived cells in recipient brains showing positive immunofluorescent staining for Iba-1, a known microglial marker (19). Microglial engraftment was observed in both the presence and absence of treatment with KA, known for inducing neuroexcitotoxic injury to the hippocampus (40, 41). The level of microglial chimerism did not appear to directly correlate with the PB engraftment rates in these transplanted mice, which ranged from 5 to 98%. Thus, in both a physiological state and in response to KA injury, transplanted GFP$^+$ cells contributed to the microglia population in the brain, with engraftment rates of GFP$^+$ donor-derived microglia into irradiated recipient mouse brains ranging from ~0.5 to 11.5% of the total resident microglia population. This is the first study known to us that proves that a single HSC, without any further manipulation or amplification in vitro, can give rise in vivo to blood lineages as well as to brain microglia when directly transplanted into a recipient adult mouse, and can form microglial nodules at the sites of CNS lesions in KA-injured

Figure 4. Laser scanning confocal micrographs of sections of brain tissue from mice transplanted with whole BM as newborns (A–J and S–V) or as adults (K–R). Tissue sections were stained with Hoechst 33342 (blue), anti-NeuN antibody (red), and anti-CD45 antibody (purple) and visualized at 63× oil (all images except D, E, I, and J) and 100× oil (D, E, I, and J). Apparent NeuN staining visualized under 63× oil objective (C and H) was found to weaken (D) or persist as faint positive NeuN staining (I) when viewed under the 100× objective (see Discussion). Images shown in A–E and S–V are taken from periventricular regions; in F–J, images are taken from the hippocampus; in K–N, images are taken from a location that included leptomeninges; and in O–R, images are taken from the olfactory bulb. Bar, 10 μm.

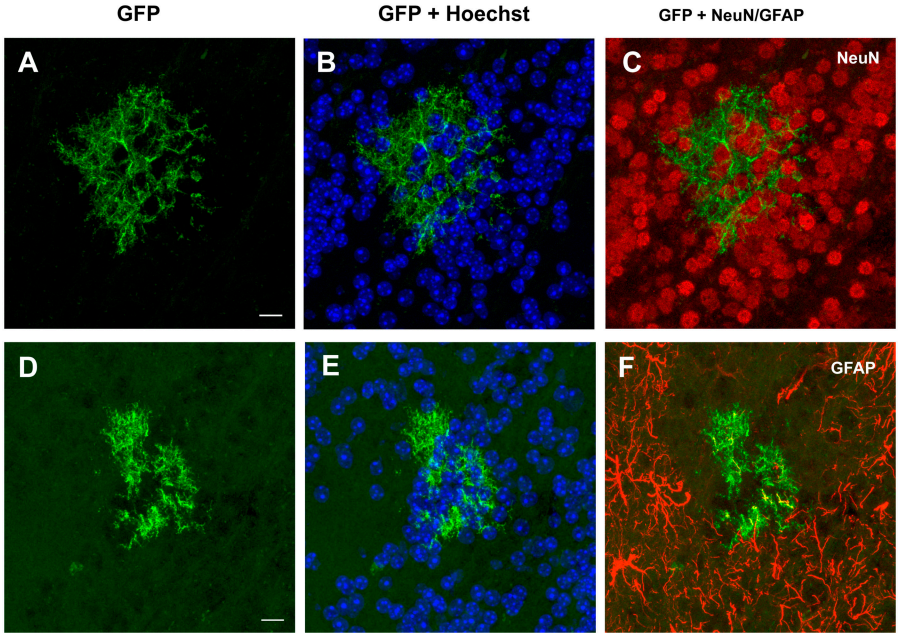

Figure 5. Laser scanning confocal micrographs showing donor marker expression in an arborizing structure consistent with an apparent cell process in the olfactory bulb of a whole BM–transplanted mouse (transplanted at birth). Tissues were stained for anti-GFP antibody (A–C, green); Hoechst 33342 (B and D, blue), and either anti-NeuN (C) or anti-GFAP antibodies (F). The green signal in D–F represents native fluorescence of GFP without amplification. Images in A–C and D–F are separated by 32 μm of tissue. Bar, 10 μm.

brains. Our data are consistent with HSCs representing the functional component in the BM responsible for giving rise to microglia. Significantly, microglial engraftment was also observed in parabiotic mice, and did not depend on brain injury, demonstrating that circulating PB cells can enter the brain and contribute to the resident microglial population without irradiation of the host. Thus, microglia appear normally to be recruited at a very low rate from circulation. The ability of such a population of blood cells to communicate between the adult hematopoietic system and brain parenchyma may have potential therapeutic implications as a vehicle for gene therapy or other treatment modalities, particularly in the treatment of CNS diseases resulting from aberrant microglia metabolism; however, the relatively low rate of engraftment observed in both transplanted and parabiotic animals currently remains a significant potential limitation to the immediate utility of such approaches.

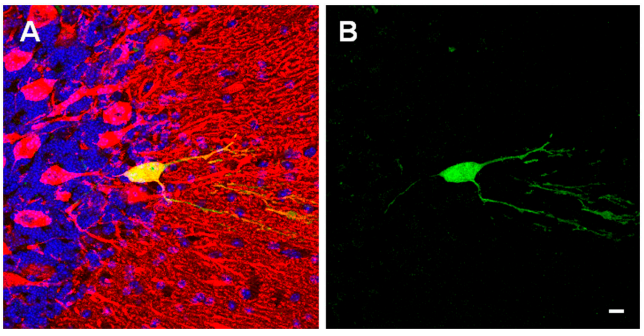

Figure 6. Laser scanning confocal micrographs showing a GFP$^+$ Purkinje cell. Tissues were stained with anti-Calbindin antibody (A, red) and Hoechst 33342 (A, blue). GFP signal (A and B, green) is endogenous and unamplified.

Rarity of nonmicroglial, nonhematopoietic fates of donor-derived HSCs

Our data indicate that the majority of donor-marker–expressing cells, other than microglia, that are present after transplantation of BM and HSCs maintain their hematopoietic identities, as illustrated by positive immunoreactivity with the panhematopoietic marker, CD45. Many microglia also maintained CD45 expression. In our study, the rare population of cells negative for both CD45 and microglial markers (Mac-1 or Iba-1) were all found to exhibit both cellular and nuclear morphology typical of microglia (Fig. 3 and not depicted). It is possible that antibodies are not sensitive enough to react with 100% of the microglia or hematopoietic cells in the section. Alternatively, hematopoietic-specific protein expression may be reduced on hematopoietic cells that cross the blood–brain barrier into brain parenchyma, where the local cellular environment is different from vascular system. This possibility has been suggested in other studies, which characterize microglia as CD45^{low} (42).

In all the animals we studied, including the parabiotic model, we were unable to confirm the existence of a BM-derived population of neurons in the olfactory bulb, as observed by others (1, 2, 7, 16). One frequent pattern we ob-

Table III. Frequency of GFP$^+$ cells in the brains of transplanted or parabiotic mice expressing neural lineage markers

Engraftment model	Animal no.	Age at transplant or parabiosis	No. of cells transplanted	Duration of survival after transplant/ parabiosis	Injury model	Blood chimerism at death (% GFP$^+$ PB cells)	No. GFP$^+$ Purkinje cells (calbindin$^+$ GFP$^+$ mormorphologically identified cells/ total GFP$^+$ cells)	No. GFP$^+$ neurons		No. GFP$^+$ astrocytes[a] (GFP$^+$GFAP$^+$/ total GFP$^+$ cells)
								Markers evaluated	No. of qualifying cells/ total GFP$^+$ cells	
WBM transplant	1	newborn	10^6	9 mo	no injury	13	1/1,099	NeuN$^+$, CD45$^-$	0/412	0/209
	2	newborn	10^6	9 mo	no injury	5	5/1,287	NeuN$^+$, CD45$^-$	0/451	0/182
	3	adult	10^6	3 mo	no injury	88	0/600	NeuN$^+$, CD45$^-$, Mac$^-$	0/291	0/310
	4	adult	10^6	3 mo	no injury	63	0/680	NeuN$^+$, CD45$^-$, Mac$^-$	0/385	0/295
	5	adult	10^6	6.5 mo	KA	92	0/429	NeuN$^+$, CD45$^-$, Mac1$^-$	0/198	0/231
	6	adult	10^6	7 mo	KA	94	0/1,065	NeuN$^+$, CD45-	0/1,010	0/55
HSC transplant	8	adult	1	3 mo	no injury	72	0/538	NeuN$^+$, CD45-, Mac1$^-$	0/105	0/65
	19	adult	100	5 mo	running	98	0/259	NeuN$^+$, CD45$^-$	0/259	ND
	20	adult	100	5 mo	running	98	0/161	NeuN$^+$, CD45$^-$	0/161	ND
	9	adult	1	4.5 mo	KA	27	0/183	NeuN$^+$, CD45$^-$	0/42	0/51
	10[b]	adult	1	9 mo	KA	98	0/710	NeuN$^+$, CD45$^-$	0/655	0/55
Parabiosis	21[c]	adult	NA	7 mo	no injury	46	0/16	NeuN$^+$, CD45$^-$	0/14	0/2
	17	adult	NA	3 mo	KA	41	0/79	NeuN$^+$, CD45$^-$	0/62	0/17

[a]The number of GFP$^+$ cells per section evaluated in the GFAP study was estimated from the average number of GFP$^+$ cells in several representative sections from the same animal.
[b]This animal received 2×10^6 unfractionated BM cells from an animal previously transplanted with a single HSC.
[c]Animal 21 was injected intramuscularly with cardiotoxin 8 wk before being killed, which has no known effects on the brain.
NA, not applicable.

served was the apparent positive colocalization of NeuN with GFP under low magnification. However, under higher magnification, NeuN reactivity was reduced to a thin rim on the cell surface. Such cells also uniformly coexpressed CD45 or Mac1. Other GFP$^+$ cells that showed positive, but very weak NeuN staining, even under the highest possible magnification, were also invariably CD45 or Mac1 positive. The aforementioned GFP$^+$ cells further exhibited morphology typical of blood cells (i.e., round cells with surface spicules or with elongated nuclei typical of microglia). Although some studies in the literature showed some GFP$^+$ cells with stronger apparent NeuN staining, the experimental conditions in those studies typically involved prolonged secondary antibody exposure or used secondary amplification protocols to increase the intensity of the observed signal. When amplifying what might be subthreshold signal, we feel it is necessary to also examine the nuclear morphology or apply other restrictive and defining markers such as CD45 to accurately identify a particular cell type.

By morphological analysis, we found one extensive arborizing structure, suggestive of a neuronal or glial subtype (Fig. 5), in the olfactory bulb of an animal transplanted with whole BM at birth. A remnant of this arborizing structure showing a smaller size was observed on another section 32 μm away from the initial section. The fragments of this putative cell captured in these two sections were both negative for CD45 (unpublished data). Despite using confocal microscopy with highest resolution and thinnest optical sections, we could not determine whether the latter section showing the smaller processes reflects true but low immunoreactivity of GFAP or an artifact, or possibly results from close proximity of surrounding GFAP$^+$ cells. No other cells were found to coexpress GFP and GFAP in the animals analyzed (Table III). As the cell body was not located, we could not perform further analysis to study its nucleus, and cannot offer evidence as to the true identity of this cell, or whether it arose as a result of cell fusion or differentiation of a GFP$^+$ cell.

Based on our data, we conclude that HSCs and their progeny largely maintain restricted cell fates after entering the brain. The vast majority of blood cells that enter brain in adults become microglia or exhibit other hematopoietic cell fates, as evidenced by CD45 or Mac1 expression. Out of 21 animals and >10,000 GFP positive cells we analyzed, both by morphology and by marker studies, we found only one possible neuronal or glial phenotype outside the cerebellum, in an animal that was transplanted with whole BM as a newborn. Occurrence at a frequency of 1/21 animals and 1/10,000 donor-marker–expressing cells is an extremely rare

event, and calls into question the importance of such phenomena to normal homeostasis and physiological or therapeutic cell replacement in the adult CNS.

MATERIALS AND METHODS

Animals. C57BL/Ka, C57BL/Ka-Thy-1.1, and C57BL/Ka-Ly5.2/Thy-1.1 mouse strains were bred and maintained at the Stanford University Research Animal Facility. eGFP-transgenic mice were generated by us as described previously (43), and were backcrossed for at least 10 generations to C57BL/Ka-Thy-1.1 mice. GFP-transgenic mice used as BM donors in these studies were 6–12 wk old. Nontransgenic C57BL/Ka mice were transplanted either at birth (postnatal days 0 or 1) or as adults, at 8–16 wk of age. For parabiosis, animals were joined at 6–10 wk of age. Mice were killed at 3–12 mo after transplant and 8–15 d after KA injury, where applicable, by intracardiac perfusion, performed under anesthesia (avertin 15 μl/g body weight), with 20 ml of 10mM EDTA followed by 20 ml of 2–4% paraformaldehyde. Animal care and experimental protocols were performed in accordance with procedures and guidelines established by the Stanford University Administrative Panel for Lab Animal Care for the humane care and use of animals.

BM harvesting. BM cells were flushed from femurs and tibiae of donor mice with a 1-ml syringe and 21-gauge needle containing HBSS (Invitrogen) supplemented with 2% FCS. Red blood cells subsequently were lysed by a 3-min incubation in 0.15 M ammonium chloride and 0.01 M potassium bicarbonate solution on ice. Leukocytes were counted on a hemocytometer and used for transplantation or for HSC staining and sorting (see next paragraph).

FACS of HSCs. GFP^+ HSCs were isolated by double FACS sorting of c-kit–enriched BM from GFP-transgenic mice, based on previously defined reactivity for particular cell surface markers (KTLS; references 44–46) as described previously (47). All antibody incubations were performed on ice for 15–25 min. BM cells were first stained with purified lineage antibodies, including KT31.1 (anti-CD3), GK1.5 (anti-CD4), 53–7.3 (anti-CD5), 53–6.7 (anti-CD8), Ter119 (antierythrocyte-specific antigen), 6B2 (anti-B220), 8C5 (anti–Gr-1), and M1/70 (anti–Mac-1), followed by anti–rat Cy5PE (Caltag). Lineage-stained cells were further stained for c-kit with biotinylated 3C11 and c-kit–positive cells were enriched by positive selection using MACS (Miltenyi Biotec) streptavidin-conjugated magnetic beads and AutoMACS cell separator columns according to manufacturer's instructions. c-kit–enriched cells were stained with fluorescently labeled 2B8 (anti–c-kit), 19XE5 (anti-Thy1.1), and E13-161.7 (anti–Sca-1) monoclonal antibodies to identify HSCs. 3C11 and 2B8 recognize distinct, nonoverlapping epitopes of c-kit. Before FACS analysis, cells were suspended in 1 μg/ml of propidium iodide to identify and exclude dead (propidium $iodide^+$) cells. KTLS HSC populations were double sorted to ensure purity, using a highly modified Vantage SE (BD Biosciences), provided by the Stanford University Shared FACS Facility. Flow cytometry data was analyzed using FlowJo (Treestar) analysis software.

Hematopoietic cell transplantation. Adult C57BL/Ka recipient mice received a lethal dose of irradiation (950 rad, delivered in a split dose 3 h apart) before transplantation by retroorbital injection with GFP^+ cells isolated from donor mice carrying the eGFP transgene, driven by the β-actin promoter (43, 48). Newborn animals were preconditioned with a sublethal dose of irradiation (400 rad, delivered in a split dose 3 h apart) before transplant via intrahepatic injection. Both adult and newborn recipient mice were transplanted with 10^6–5×10^7 GFP^+ BM cells, or with 1 or 100 FACS-purified GFP^+ KTLS HSCs. B cells, T cells, and myeloid cells in the PB of reconstituted animals were identified by flow cytometry using anti-B220, anti-CD3, or anti–Mac-1/anti–Gr-1, respectively. All transplanted mice analyzed in these studies showed significant levels of multilineage chimerism of PB leukocytes, as indicated in Tables I–III.

Parabiosis. Parabiosis surgery was performed exactly as described previously (30), and in accordance with the guidelines established by the Stanford University Administrative Panel for Lab Animal Care for the humane care and use of animals.

KA injury. To induce injury to hippocampal neurons, some animals were treated with KA. For transplanted animals, KA was administered 2–4 mo after transplant, whereas for parabiotic animals, KA was given 24 h before parabiosis. Animals were first anesthetized using 3% isofluorane before intraperitoneal injection of 20 mg/kg KA (Sigma-Aldrich) prepared at 10 mg/ml in sterile PBS. Animals were warmed and observed for up to 8 h after KA injection. In all KA-treated animals, seizures began ~5–10 min after injection, and recurred for a period of up to 3 h. Responses of individual animals to KA injection were scored every 5 min for the first 2 h and every 15 min for the next 2 h as follows: 0, no effect; 1, arrest of motion; 2, myoclonic jerks of the head and neck, with brief twitching movements; 3, unilateral clonic activity; 4, bilateral forelimb tonic and clonic activity; and 5, generalized tonic-clonic activity with loss of postural tone including death from continuous convulsions, as described previously (40, 41). Mortality among all KA-treated animals was ~30%. Animals that survived KA treatment showed a similar range of seizure grades, generally between grades 2 and 5 in the first 2 h after injection.

Running wheel exercise. In some experiments, mice were provided with running wheels for a period of 28 d before being killed. Mice were observed to engage in this exercise readily and voluntarily.

Immunofluorescence. After perfusion, brains were harvested from control, transplanted, or parabiotic animals and subsequently fixed in 2–4% paraformaldehyde overnight, followed by cryopreservation in 30% sucrose at 4°C until submerged (usually overnight). Cryostat sagittal sections, including the olfactory bulb, cortex, and cerebellum, were cut at a 5–16-μm thickness and placed onto Superfrost/Plus slides, dehydrated, and stored at −80°C until use. Citrate buffer and heat antigen retrieval was performed on sections for NeuN staining per standard protocol. Sections were permeabilized and blocked in 3% goat serum with 0.3% Triton X-100 and stained with primary antibodies at room temperature for 1–3 h or at a 4°C for 16–48 h in light-protected humid chambers. Mouse-on-mouse (MOM) immunodetection kit (Vector Laboratories) was used for staining with antibodies raised in mouse. Primary antibodies used included mouse anti-NeuN (Chemicon International), mouse anti-MAP2 (Chemicon), 1:400; rabbit anticalbindin (Chemicon), 1:400; rabbit anti–cow GFAP (DakoCytomation), polyclonal, 1:2,000; rat anti-Mac1 (eBioscience), 1:50; rabbit anti-Iba1 (a gift from Y. Imai, National Institute of Neuroscience, Tokyo, Japan), polyclonal, 1:600; rat anti-CD45 (BD Biosciences), 1:100; and rabbit anti-GFP conjugated with Alexa Fluor-488 (Molecular Probes), 1:250. Secondary antibodies used included goat anti–mouse conjugated with Alexa Fluor-594, goat anti–rabbit conjugated with Alexa Fluor-594, and goat anti–rat conjugated with Alexa-594 or Alexa Fluor-633 (Molecular Probes). Nuclei were stained with Hoechst 1:1,000 (Molecular Probes). Stained sections were analyzed for coexpression of the indicated markers by confocal microscopy. This analysis typically included all fields of the sagittal brain sections, representing olfactory bulb, cortex, cerebellum, choroid plexus, and periventricular (including subventricular) regions of the brain.

Confocal microscopy. Images were collected using a 63× (N.A 1.4) or 100× (N.A. 1.4) oil immersion on a Leica SP2 AOBS or a Zeiss LSM510 laser scanning confocal microscope as indicated. On the Leica system, zooming was performed during the optical data collection using a pin hole size of 1 Airy unit, and the optimal Z axis step size (as indicated by the software) was used to collect data for Z stack series. Images were processed with Adobe Photoshop for presentation.

The authors wish to thank L. Jerabek for laboratory management, R. Sherwood and Dr. T. Serwold for their assistance in FACS analysis, Dr. Y. Imai for the gift of Iba1

antibody, Dr. J. Mulholland for helpful discussions, and the Stanford University Medical Center Cell Science Imaging Facility.

This work was supported in part through National Institutes of Health grant no. CA86065 (to I.L. Weissman), a Burroughs Wellcome Fund Career Award (to A.J. Wagers), and a grant from Stanford University School of Medicine Medical Scholar Program (to M. Massengale).

Affiliations that might be perceived to have biased this work are as follows. I.L. Weissman was a member of the SAB of Amgen and owns significant Amgen stock. I.L. Weissman cofounded and consulted for Systemix, is a cofounder and director of Stem Cells, Inc., and recently cofounded Cellerant, Inc. The authors have no other potential conflicting financial interests.

Submitted: 3 January 2005
Accepted: 1 April 2005

REFERENCES

1. Brazelton, T.R., F.M. Rossi, G.I. Keshet, and H.M. Blau. 2000. From marrow to brain: expression of neuronal phenotypes in adult mice. *Science*. 290:1775–1779.
2. Mezey, E., K.J. Chandross, G. Harta, R.A. Maki, and S.R. McKercher. 2000. Turning blood into brain: cells bearing neuronal antigens generated in vivo from bone marrow. *Science*. 290:1779–1782.
3. Black, I.B., and D. Woodbury. 2001. Adult rat and human bone marrow stromal stem cells differentiate into neurons. *Blood Cells Mol. Dis*. 27:632–636.
4. Cogle, C.R., A.T. Yachnis, E.D. Laywell, D.S. Zander, J.R. Wingard, D.A. Steindler, and E.W. Scott. 2004. Bone marrow transdifferentiation in brain after transplantation: a retrospective study. *Lancet*. 363: 1432–1437.
5. Kabos, P., M. Ehtesham, A. Kabosova, K.L. Black, and J.S. Yu. 2002. Generation of neural progenitor cells from whole adult bone marrow. *Exp. Neurol*. 178:288–293.
6. Munoz-Elias, G., D. Woodbury, and I.B. Black. 2003. Marrow stromal cells, mitosis, and neuronal differentiation: stem cell and precursor functions. *Stem Cells*. 21:437–448.
7. Munoz-Elias, G., A.J. Marcus, T.M. Coyne, D. Woodbury, and I.B. Black. 2004. Adult bone marrow stromal cells in the embryonic brain: engraftment, migration, differentiation, and long-term survival. *J. Neurosci*. 24:4585–4595.
8. Mezey, E., S. Key, G. Vogelsang, I. Szalayova, G.D. Lange, and B. Crain. 2003. Transplanted bone marrow generates new neurons in human brains. *Proc. Natl. Acad. Sci. USA*. 100:1364–1369.
9. Priller, J., D.A. Persons, F.F. Klett, G. Kempermann, G.W. Kreutzberg, and U. Dirnagl. 2001. Neogenesis of cerebellar Purkinje neurons from gene-marked bone marrow cells in vivo. *J. Cell Biol*. 155:733–738.
10. Takizawa, S. 2003. Differentiation of adult bone marrow cells into neurons and endothelial cells in rat brain after stroke in the presence of cytokines. [In Japanese.] *Rinsho Shinkeigaku*. 43:830–831.
11. Torrente, Y., M. Belicchi, F. Pisati, S.F. Pagano, F. Fortunato, M. Sironi, M.G. D'Angelo, E.A. Parati, G. Scarlato, and N. Bresolin. 2002. Alternative sources of neurons and glia from somatic stem cells. *Cell Transplant*. 11:25–34.
12. Woodbury, D., E.J. Schwarz, D.J. Prockop, and I.B. Black. 2000. Adult rat and human bone marrow stromal cells differentiate into neurons. *J. Neurosci. Res*. 61:364–370.
13. Zhao, Y., D. Glesne, and E. Huberman. 2003. A human peripheral blood monocyte-derived subset acts as pluripotent stem cells. *Proc. Natl. Acad. Sci. USA*. 100:2426–2431.
14. Eglitis, M.A., and E. Mezey. 1997. Hematopoietic cells differentiate into both microglia and macroglia in the brains of adult mice. *Proc. Natl. Acad. Sci. USA*. 94:4080–4085.
15. Sanchez-Ramos, J., S. Song, F. Cardozo-Pelaez, C. Hazzi, T. Stedeford, A. Willing, T.B. Freeman, S. Saporta, W. Janssen, N. Patel, et al. 2000. Adult bone marrow stromal cells differentiate into neural cells in vitro. *Exp. Neurol*. 164:247–256.
16. Corti, S., F. Locatelli, S. Strazzer, S. Salani, R. Del Bo, D. Soligo, P. Bossolasco, N. Bresolin, G. Scarlato, and G.P. Comi. 2002. Modulated generation of neuronal cells from bone marrow by expansion and mobilization of circulating stem cells with in vivo cytokine treatment. *Exp. Neurol*. 177:443–452.
17. Wagers, A.J., and I.L. Weissman. 2004. Plasticity of adult stem cells. *Cell*. 116:639–648.
18. Trowbridge, I.S., and M.L. Thomas. 1994. CD45: an emerging role as a protein tyrosine phosphatase required for lymphocyte activation and development. *Annu. Rev. Immunol*. 12:85–116.
19. Ito, D., Y. Imai, K. Ohsawa, K. Nakajima, Y. Fukuuchi, and S. Kohsaka. 1998. Microglia-specific localisation of a novel calcium binding protein, Iba1. *Brain Res. Mol. Brain Res*. 57:1–9.
20. Mullen, R.J., C.R. Buck, and A.M. Smith. 1992. NeuN, a neuronal specific nuclear protein in vertebrates. *Development*. 116:201–211.
21. van Praag, H., G. Kempermann, and F.H. Gage. 1999. Running increases cell proliferation and neurogenesis in the adult mouse dentate gyrus. *Nat. Neurosci*. 2:266–270.
22. van Praag, H., B.R. Christie, T.J. Sejnowski, and F.H. Gage. 1999. Running enhances neurogenesis, learning, and long-term potentiation in mice. *Proc. Natl. Acad. Sci. USA*. 96:13427–13431.
23. Mizumatsu, S., M.L. Monje, D.R. Morhardt, R. Rola, T.D. Palmer, and J.R. Fike. 2003. Extreme sensitivity of adult neurogenesis to low doses of X-irradiation. *Cancer Res*. 63:4021–4027.
24. Monje, M.L., and T. Palmer. 2003. Radiation injury and neurogenesis. *Curr. Opin. Neurol*. 16:129–134.
25. Monje, M.L., H. Toda, and T.D. Palmer. 2003. Inflammatory blockade restores adult hippocampal neurogenesis. *Science*. 302:1760–1765.
26. Alvarez-Dolado, M., R. Pardal, J.M. Garcia-Verdugo, J.R. Fike, H.O. Lee, K. Pfeffer, C. Lois, S.J. Morrison, and A. Alvarez-Buylla. 2003. Fusion of bone-marrow-derived cells with Purkinje neurons, cardiomyocytes and hepatocytes. *Nature*. 425:968–973.
27. Weimann, J.M., C.B. Johansson, A. Trejo, and H.M. Blau. 2003. Stable reprogrammed heterokaryons form spontaneously in Purkinje neurons after bone marrow transplant. *Nat. Cell Biol*. 5:959–966.
28. Weimann, J.M., C.A. Charlton, T.R. Brazelton, R.C. Hackman, and H.M. Blau. 2003. Contribution of transplanted bone marrow cells to Purkinje neurons in human adult brains. *Proc. Natl. Acad. Sci. USA*. 100:2088–2093.
29. Bunster, E., and R.K. Meyer. 1933. An improved method of parabiosis. *Anat. Rec*. 57:339–343.
30. Wright, D.E., A.J. Wagers, A.P. Gulati, F.L. Johnson, and I.L. Weissman. 2001. Physiological migration of hematopoietic stem and progenitor cells. *Science*. 294:1933–1936.
31. Wagers, A.J., R.I. Sherwood, J.L. Christensen, and I.L. Weissman. 2002. Little evidence for developmental plasticity of adult hematopoietic stem cells. *Science*. 297:2256–2259.
32. Vallieres, L., and P.E. Sawchenko. 2003. Bone marrow-derived cells that populate the adult mouse brain preserve their hematopoietic identity. *J. Neurosci*. 23:5197–5207.
33. Priller, J., A. Flugel, T. Wehner, M. Boentert, C.A. Haas, M. Prinz, F. Fernandez-Klett, K. Prass, I. Bechmann, B.A. de Boer, et al. 2001. Targeting gene-modified hematopoietic cells to the central nervous system: use of green fluorescent protein uncovers microglial engraftment. *Nat. Med*. 7:1356–1361.
34. Ling, E.A., and W.C. Wong. 1993. The origin and nature of ramified and amoeboid microglia: a historical review and current concepts. *Glia*. 7:9–18.
35. Hess, D.C., T. Abe, W.D. Hill, A.M. Studdard, J. Carothers, M. Masuya, P.A. Fleming, C.J. Drake, and M. Ogawa. 2004. Hematopoietic origin of microglial and perivascular cells in brain. *Exp. Neurol*. 186: 134–144.
36. Flugel, A., M. Bradl, G.W. Kreutzberg, and M.B. Graeber. 2001. Transformation of donor-derived bone marrow precursors into host microglia during autoimmune CNS inflammation and during the retrograde response to axotomy. *J. Neurosci. Res*. 66:74–82.
37. Hickey, W.F., and H. Kimura. 1988. Perivascular microglial cells of the CNS are bone marrow-derived and present antigen in vivo. *Science*. 239:290–292.
38. Del Rio-Hortega, P. 1932. Microglia. Cytology & Cellular Pathology

of the Nervous System. Paul B. Hoeber, Inc., New York. 483–534 pp.
39. Kaur, C., A.J. Hao, C.H. Wu, and E.A. Ling. 2001. Origin of microglia. *Microsc. Res. Tech.* 54:2–9.
40. Yang, D.D., C.Y. Kuan, A.J. Whitmarsh, M. Rincon, T.S. Zheng, R.J. Davis, P. Rakic, and R.A. Flavell. 1997. Absence of excitotoxicity-induced apoptosis in the hippocampus of mice lacking the Jnk3 gene. *Nature.* 389:865–870.
41. Yoshimura, S., Y. Takagi, J. Harada, T. Teramoto, S.S. Thomas, C. Waeber, J.C. Bakowska, X.O. Breakefield, and M.A. Moskowitz. 2001. FGF-2 regulation of neurogenesis in adult hippocampus after brain injury. *Proc. Natl. Acad. Sci. USA.* 98:5874–5879.
42. Sedgwick, J.D., S. Schwender, H. Imrich, R. Dorries, G.W. Butcher, and V. ter Meulen. 1991. Isolation and direct characterization of resident microglial cells from the normal and inflamed central nervous system. *Proc. Natl. Acad. Sci. USA.* 88:7438–7442.
43. Wright, D.E., S.H. Cheshier, A.J. Wagers, T.D. Randall, J.L. Christensen, and I.L. Weissman. 2001. Cyclophosphamide/granulocyte colony-stimulating factor causes selective mobilization of bone marrow hematopoietic stem cells into the blood after M phase of the cell cycle. *Blood.* 97:2278–2285.
44. Morrison, S.J., A.M. Wandycz, H.D. Hemmati, D.E. Wright, and I.L. Weissman. 1997. Identification of a lineage of multipotent hematopoietic progenitors. *Development.* 124:1929–1939.
45. Morrison, S.J., and I.L. Weissman. 1994. The long-term repopulating subset of hematopoietic stem cells is deterministic and isolatable by phenotype. *Immunity.* 1:661–673.
46. Spangrude, G.J., S. Heimfeld, and I.L. Weissman. 1988. Purification and characterization of mouse hematopoietic stem cells. *Science.* 241:58–62.
47. Wagers, A.J., R.C. Allsopp, and I.L. Weissman. 2002. Changes in integrin expression are associated with altered homing properties of Lin(−/lo)Thy1.1(lo)Sca-1(+)c-kit(+) hematopoietic stem cells following mobilization by cyclophosphamide/granulocyte colony-stimulating factor. *Exp. Hematol.* 30:176–185.
48. Okabe, M., M. Ikawa, K. Kominami, T. Nakanishi, and Y. Nishimune. 1997. 'Green mice' as a source of ubiquitous green cells. *FEBS Lett.* 407:313–319.